

# Simultaneous Dual-Frequency, Round-Trip Calibration of Doppler Data With Application to Radio Science Experiments

A. L. Berman  
TDA Engineering Office

*Simultaneous dual-frequency, round-trip (uplink and downlink) calibration of Doppler data is expected to be a requirement of several radio science experiments being planned for the next decade, and such (calibration) capability is expected to be achieved by the mid-1980s. Simultaneous dual-frequency, round-trip calibration would be straightforward except for the condition of unequal spacecraft turnaround ratios at S- and X-band. This article discusses the impact of unequal turnaround ratios on calibration accuracies in the specific cases of the Gravitational Wave Detection Experiment and the Solar Gravitational Quadrupole Moment Experiment.*

## I. Introduction

By the early to mid-1980s, the Deep Space Network (DSN) is expected to have augmented the current S-band uplink capability with X-band uplink capability. With additional modification to the spacecraft and ground tracking system, one can readily foresee the provision of the capability for simultaneous round-trip (uplink and downlink) transmission of S- and X-band frequencies. Simultaneous (and independent) transmission of S- and X-band frequency provides the important capability of high-precision calibration of charged particle effects on radio metric (i.e., Doppler and range) data. This new capability will be crucial to certain radio science experiments, and may additionally prove to be beneficial in regard to navigational usage of radio metric data. Such round-trip, dual-frequency calibrations would be (close to) exact and trivial to apply, except for the fact that the spacecraft turnaround ratios<sup>1</sup> at S- and X-band are, according to the current design, expected to be (slightly) unequal.

Simultaneous dual-frequency<sup>2</sup> calibration of radio metric data is expected to be important to the following radio science experiments:

Radio science experiment	Sun-Earth-probe angle, deg	Radio metric data type of interest
Gravitational Wave Detection	~ 180	Doppler
Relativity Tests	~ 0	Range
Solar Quadrupole Measurement	~ 0	Doppler

Callahan (Ref. 1) has treated simultaneous dual-frequency calibration of range data. Although the mechanics of the calibration are similar for both the Doppler and range applica-

<sup>1</sup>Ratio of spacecraft transmitted frequency to spacecraft received frequency for a single-frequency band.

<sup>2</sup>"Simultaneous dual-frequency" will specifically imply "simultaneous, independent, round-trip, dual-frequency."

tions, the final efficacy of the calibration in any given application is highly dependent upon the particular circumstances of the application.

This article will derive and discuss simultaneous dual-frequency calibration of Doppler data. Specifically emphasized will be the application of simultaneous dual-frequency calibration of Doppler data in regard to the Gravitational Wave Detection Experiment (Ref. 2) and the Solar Quadrupole Moment Experiment (Ref. 3).

## II. Simultaneous Dual-Frequency, Round-Trip Calibration of Doppler Data

It was noted in Section I that the main difficulty with simultaneous dual-frequency calibration capability is that the spacecraft turnaround ratios at S- and X-band are expected to be (slightly) unequal. Figure 1 presents a simplified block diagram of dual-frequency transmission; the relevant parameters are defined as follows:

$$F_0 = \text{S-band uplink frequency} \\ \approx 2.115 \text{ GHz}$$

$$K_0 = \text{ratio of uplink X-band to uplink S-band} \\ \approx 3.404$$

$$C_0 = \text{S-band spacecraft turnaround ratio} \\ \approx 1.086$$

$$C_1 = \text{X-band spacecraft turnaround ratio} \\ \approx 1.169$$

One now makes the following additional definitions (where  $\Delta\phi$  relates to columnar electron (number) density fluctuation):

Uplink charged particle fluctuation effect (in cycles)

$$= \Delta\phi_{\text{up}} \left( \frac{F_0 C_0}{f} \right)$$

Downlink charged particle fluctuation effect (in cycles)

$$= \Delta\phi_{\text{dn}} \left( \frac{F_0 C_0}{f} \right)$$

$f$  = frequency

To isolate the frequency-dependent effects (i.e., charged particle fluctuation effects), one scales the downlink X-band by the downlink S-X ratio ( $C_0/C_1 K_0$ ) and differences this with the

downlink S-band. The quantity being operated on is integrated (counted) Doppler frequency during a given (averaging time) interval:

$$\Delta\phi_m \equiv \text{measured charged particle fluctuation effect, in cycles (at S-band downlink frequency)} \\ = \left[ F_s - \left( \frac{C_0}{C_1 K_0} \right) F_x \right]$$

where:

$$F_s = \text{(integrated) S-band downlink frequency}$$

$$F_x = \text{(integrated) X-band downlink frequency}$$

In terms of  $\Delta\phi_{\text{up}}$  and  $\Delta\phi_{\text{dn}}$ , one expects for the measured charged particle fluctuation effect:

$$\Delta\phi_m = \left[ \Delta\phi_{\text{up}} \left( \frac{F_0 C_0}{F_0} \right) \cdot C_0 + \Delta\phi_{\text{dn}} \left( \frac{F_0 C_0}{F_0 C_0} \right) \right. \\ \left. - \left( \frac{C_0}{C_1 K_0} \right) \cdot \left[ \Delta\phi_{\text{up}} \left( \frac{F_0 C_0}{K_0 F_0} \right) \cdot C_1 \right. \right. \\ \left. \left. + \Delta\phi_{\text{dn}} \left( \frac{F_0 C_0}{C_1 K_0 F_0} \right) \right] \right] \\ = \Delta\phi_{\text{up}} C_0^2 \left[ 1 - \frac{1}{K_0^2} \right] + \Delta\phi_{\text{dn}} \left[ 1 - \frac{C_0^2}{C_1^2 K_0^2} \right]$$

By defining the difference between uplink and downlink charged particle fluctuation effect:

$$\epsilon \equiv \Delta\phi_{\text{up}} - \Delta\phi_{\text{dn}}$$

one obtains the downlink charged particle fluctuation effect in terms of the measured charged particle fluctuation effect and the uplink-downlink difference:

$$\Delta\phi_{\text{dn}} = \frac{\Delta\phi_m - \epsilon C_0^2 \left( 1 - \frac{1}{K_0^2} \right)}{\left[ C_0^2 \left( 1 - \frac{1}{K_0^2} \right) + 1 - \frac{C_0^2}{C_1^2 K_0^2} \right]}$$

One now writes the expression for the measured charged particle fluctuation effect in terms of the desired (scaled) calibration (first bracketed term) and a term that is dependent on the (unknown) uplink-downlink differences (second bracketed term):

$$\Delta\phi_m = \left\{ \left[ 1 - \frac{1}{K_0^2} \right] \cdot \left( C_0^2 \Delta\phi_{up} + \Delta\phi_{dn} \right) \right\} + \left\{ \frac{1}{K_0^2} \left[ 1 - \frac{C_0^2}{C_1^2} \right] \cdot \Delta\phi_{dn} \right\}$$

The appropriate (S-band) calibration is now identified as follows:

$$\begin{aligned} C_0^2 \Delta\phi_{up} + \Delta\phi_{dn} &= \left( 1 - \frac{1}{K_0^2} \right)^{-1} \left\{ \Delta\phi_m - \frac{1}{K_0^2} \left[ 1 - \frac{C_0^2}{C_1^2} \right] \cdot \Delta\phi_{dn} \right\} \\ &= \left( 1 - \frac{1}{K_0^2} \right)^{-1} \left\{ \Delta\phi_m - \frac{\frac{1}{K_0^2} \left( 1 - \frac{C_0^2}{C_1^2} \right) \left[ \Delta\phi_m - \epsilon C_0^2 \left( 1 - \frac{1}{K_0^2} \right) \right]}{\left[ C_0^2 \left( 1 - \frac{1}{K_0^2} \right) + 1 - \frac{C_0^2}{C_1^2 K_0^2} \right]} \right\} \end{aligned}$$

Christensen (Ref. 4) first noted that dual-frequency calibration of either frequency is (essentially) equivalent; the X-band calibration corresponding to the above (S-band) calibration is:

$$C_1^2 \Delta\phi_{up} + \Delta\phi_{dn} = \left( 1 - \frac{1}{K_0^2} \right)^{-1} \left\{ \Delta\phi_m - \frac{\left( \frac{C_1^2}{C_0^2} - 1 \right) \left[ \Delta\phi_m - \epsilon C_1^2 \left( 1 - \frac{1}{K_0^2} \right) \right]}{\left[ C_1^2 \left( 1 - \frac{1}{K_0^2} \right) - \frac{1}{K_0^2} + \frac{C_1^2}{C_0^2} \right]} \right\}$$

These expressions reduce to:

$$C_0^2 \Delta\phi_{up} + \Delta\phi_{dn} \propto \Delta\phi_m + 6.40 \times 10^{-3} \epsilon \text{ (S-band)}$$

$$C_1^2 \Delta\phi_{up} + \Delta\phi_{dn} \propto \Delta\phi_m + 9.17 \times 10^{-2} \epsilon \text{ (X-band)}$$

The S-band result is similar to that obtained by Callahan (Ref. 1). To utilize these relationships, one needs to be able to relate  $\epsilon$  to  $\Delta\phi_m$ ; this can only be done in the context of specific experimental conditions. Applications of these results to specific radio science experiments will be discussed in Sections III and IV to follow.

### III. Gravitational Wave Detection Experiment Application

The gravitational wave detection experiment utilizing ultra-precise Doppler data has been described in detail in Ref. 2. The experiment is expected to be performed under the following conditions:

- (1) SEP  $\sim 180$  deg (specifically to reduce solar wind fluctuations).
- (2) Long round-trip light times (RTLts).

Under such conditions, most of the electron density (and density fluctuation) is near-Earth, so that the correlation time

of interest between uplink and downlink solar wind fluctuation is essentially the RTLTL. The Doppler sample interval of interest will be significantly less than the RTLTL (Ref. 2). Under these circumstances, one can expect little correlation between  $\Delta\phi_{up}$  and  $\Delta\phi_{dn}$ . A reasonable and quite conservative assumption to make under such conditions is that the difference between  $\Delta\phi_{up}$  and  $\Delta\phi_{dn}$  is of the same order as the quantities themselves, or, very approximately:

$$\epsilon = \Delta\phi_{up} - \Delta\phi_{dn} \sim \Delta\phi_m$$

For the X-band calibration, one thus expects an error of approximately 0.1 ( $\sim 9.17 \times 10^{-2} \epsilon/\Delta\phi_m$ ) when using simultaneous dual-frequency calibration with the currently expected unequal turnaround ratios. Since the quantity of interest to the gravitational wave detection experiment is fractional frequency fluctuation:

$$\sigma(\Delta F/F)$$

one expects a simple order-of-magnitude improvement over the performance for uncalibrated two-way X-band (uplink and downlink). Figures 2 and 3 update previous graphs (Ref. 5) of (with  $\tau_a$  = averaging time):

$$\sigma(\Delta F/F) \text{ versus } \tau_a$$

under the assumption that simultaneous dual-frequency calibrations result in an order-of-magnitude improvement for the gravitational wave detection experiment conditions.

#### IV. Solar Quadrupole Moment Experiment Application

The experiment to measure the solar gravitational quadrupole moment via a spacecraft passing very close to the Sun (for instance, at four solar radii as in the proposed Solar Probe Mission) is described by Anderson, et al., in Ref. 3. In this experiment, Doppler measurements at an approximate 10-minute sample interval are the quantity of interest. Most pertinent to the consideration of simultaneous dual-frequency calibration is that the spacecraft is (essentially) *at* the closest approach distance during the time of minimum SEP ( $\sim 1$  deg for the Solar Probe Mission), hence the spacecraft is located at the point of maximum signal path electron density (and density fluctuation). The importance of this is that for any Doppler averaging times greater than a few seconds the  $\Delta\phi_{up}$

and  $\Delta\phi_{dn}$  will be extremely well correlated. Allowing the very conservative approximation (for a 10-minute averaging time):

$$\epsilon = \Delta\phi_{up} - \Delta\phi_{dn} \sim 0.1\Delta\phi_m$$

results in an error of approximately 0.01 ( $\sim 9.17 \times 10^{-2} \epsilon/\Delta\phi_m$ ), hence one can expect a two orders-of-magnitude improvement via simultaneous dual-frequency calibration of X-band as compared to uncalibrated two-way X-band. From Ref. 3, the uncalibrated two-way X-band error at four solar radii is (solar wind fluctuation error only):

$$1\sigma = 2.5 \text{ mm/s}$$

and therefore, with simultaneous dual-frequency calibration of X-band, one can expect:

$$1\sigma = 2.5 \times 10^{-2} \text{ mm/s}$$

At the current time, the ground tracking system (rubidium frequency standard) has a frequency fluctuation of approximately (with  $\tau_a = 10$  minutes):

$$1\sigma \approx 1.0 \times 10^{-1} \text{ mm/s}$$

so that even with unequal spacecraft turnaround ratios, simultaneous dual-frequency calibrations appear to be able to reduce solar wind fluctuation in this experiment to below the current (system) inherent limitations.

#### V. Discussion and Summary

Simultaneous dual-frequency, round-trip (uplink and downlink) capability provides the crucial ability to be able to calibrate solar wind fluctuation in radio science experiments that require highly precise Doppler measurements. The calibration process is complicated by the usage (as per current design) of unequal spacecraft turnaround ratios at S- and X-band. In the case of the Gravitational Wave Detection Experiment, the unequal turnaround ratios limit the calibration to an order-of-magnitude improvement over the uncalibrated two-way (uplink and downlink) X-band; eventually this may result in solar wind fluctuation being the limiting factor in achieving increased system sensitivity. For the Solar Gravitational Quadrupole Moment Experiment, on the other hand, the unequal turnaround ratios will basically not compromise the calibration accuracy of simultaneous dual-frequency, round-trip capability.

## References

1. Callahan, P. S., "Range Accuracy as a Function of Tracking Frequencies and Calibration Strategy", IOM 315-66, 25 August 1978. (JPL internal document.)
2. Berman, A. L., "The Gravitational Wave Detection Experiment: Description and Anticipated Requirements", in *The Deep Space Network Progress Report 42-46*, Jet Propulsion Laboratory, Pasadena, California, August 15, 1978.
3. Anderson, J. D., and Lau, E. L., "Gravitational Experiments on Solar Probe", in *A Close-up of The Sun*, edited by Neugebauer, M., and Davies, R. W., JPL Publication 78-70, Jet Propulsion Laboratory, Pasadena, California, September 1, 1978.
4. Christensen, C. S., "Difference Range Error Equations for Voyager — Revisited", IOM 314-123, 1 June 1977. (JPL internal document.)
5. Berman, A. L., "Solar Wind Density Fluctuation and The Experiment to Detect Gravitational Waves in Ultraprecise Doppler Data", in *The Deep Space Network Progress Report 42-44*, Jet Propulsion Laboratory, Pasadena, California, April 15, 1978.

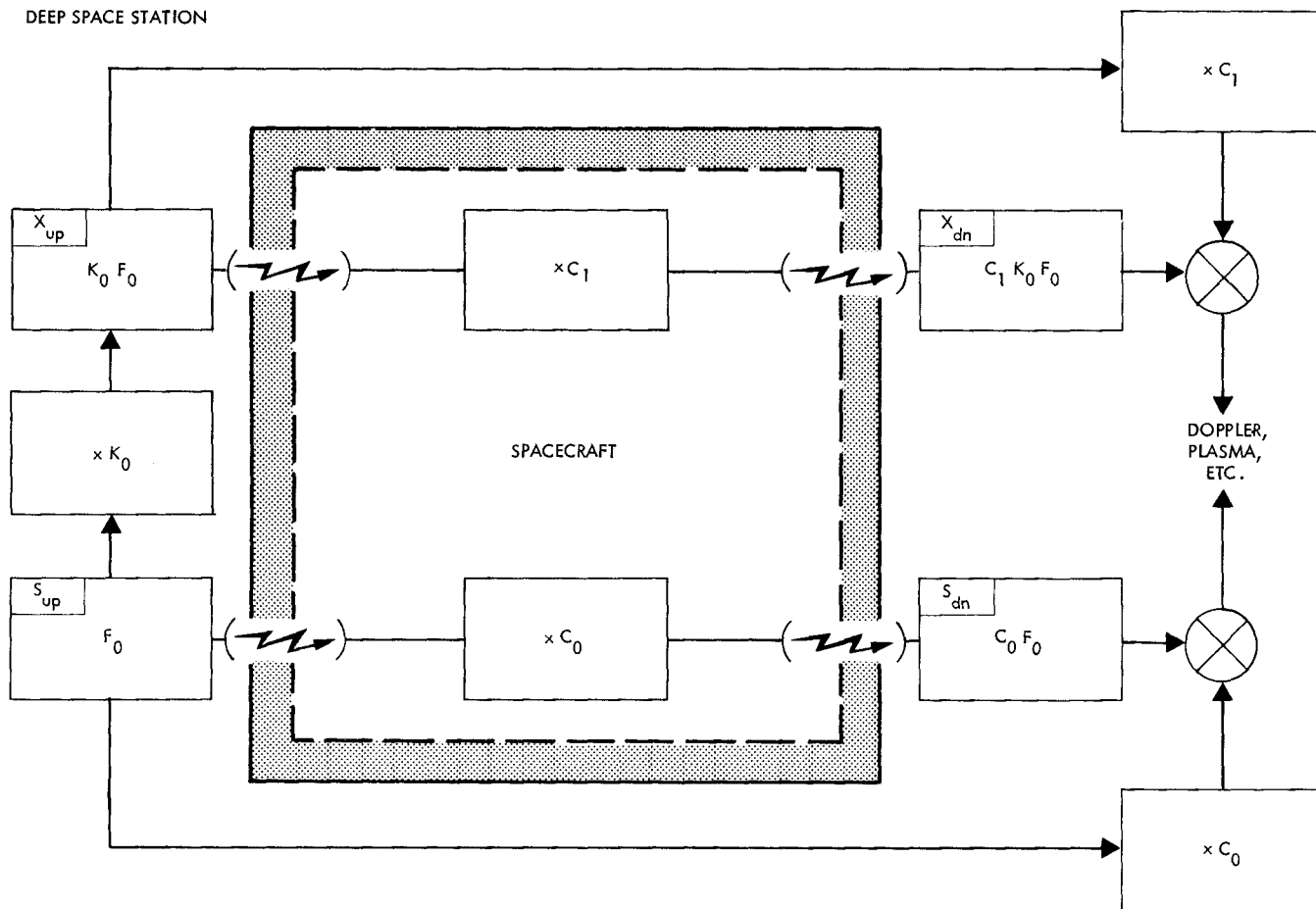


Fig. 1. Simplified functional block diagram of simultaneous dual-frequency uplink and downlink transmission ( $F_0 = 2.115$  GHz,  $K_0 \approx 3.404$ ,  $C_0 \approx 1.086$ ,  $C_1 \approx 1.196$ )

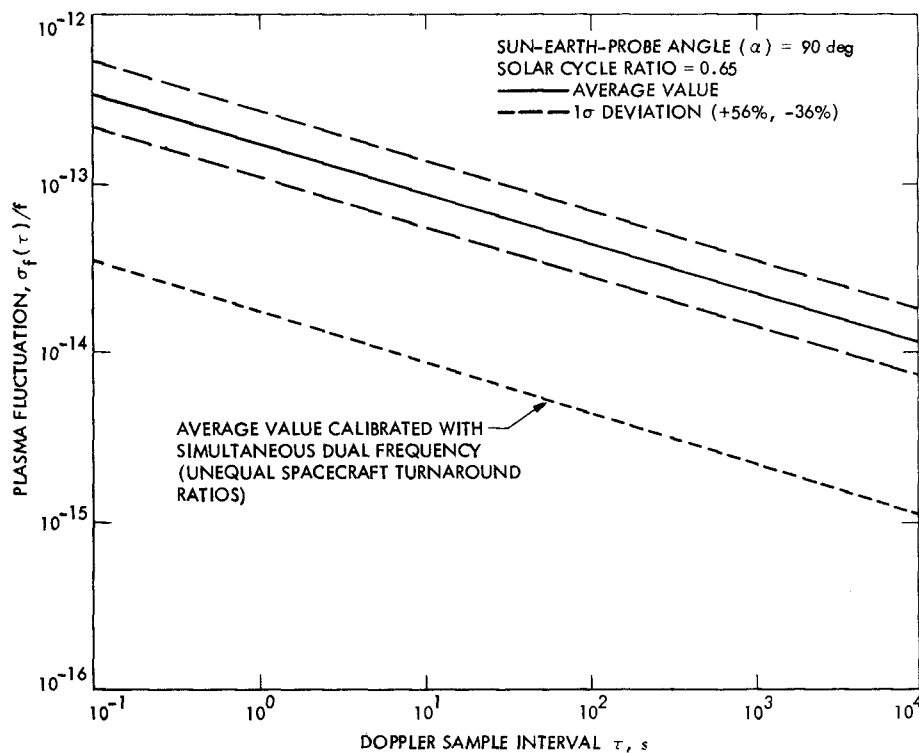


Fig. 2. Two-way X-band plasma fluctuation at solar cycle minimum

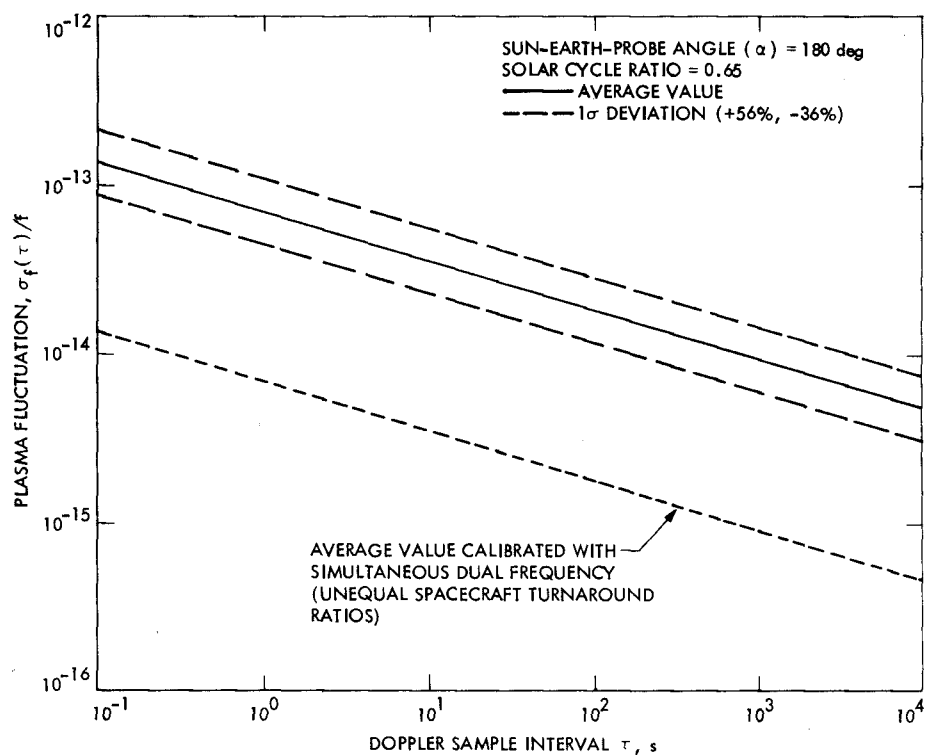


Fig. 3. Two-way X-band plasma fluctuation at solar cycle maximum